**RESEARCH ARTICLE**

WILEY

# Predictable information in neural signals during resting state is reduced in autism spectrum disorder

Alla Brodski-Guerniero[1] | Marcus J. Naumer[2] | Vera Moliadze[3,4] |
Jason Chan[2,3,5] | Heike Althen[3] | Fernando Ferreira-Santos[6] | Joseph T. Lizier[7] |
Sabine Schlitt[3] | Janina Kitzerow[3] | Magdalena Schütz[2,3] | Anne Langer[2,3] |
Jochen Kaiser[2] | Christine M. Freitag[3] | Michael Wibral[1]

[1]MEG Unit, Brain Imaging Center, Goethe University, Frankfurt am Main, Germany

[2]Institute of Medical Psychology, Faculty of Medicine, Goethe University, Frankfurt am Main, Germany

[3]Department of Child and Adolescent Psychiatry, Psychosomatics and Psychotherapy, Autism Research and Intervention Center of Excellence, University Hospital Frankfurt, Goethe University, Frankfurt am Main, Germany

[4]Department of Medical Psychology and Medical Sociology, Schleswig-Holstein University Hospital (UKSH), Christian-Albrechts-University, Kiel, Germany

[5]School of Applied Psychology, University College Cork, Cork, Ireland

[6]Laboratory of Neuropsychophysiology, Faculty of Psychology and Education Sciences, University of Porto, Porto, Portugal

[7]Complex Systems Research Group and Centre for Complex Systems, Faculty of Engineering & IT, The University of Sydney, New South Wales 2006, Australia

**Correspondence**
Alla Brodski-Guerniero, MEG Unit, Brain Imaging Center, Heinrich-Hoffmann-Straße 10, 60528 Frankfurt am Main, Germany.
Email: alla@brodski.de

**Funding information**
Ernst Ludwig Ehrlich Studienwerk (BMBF Scholarship for Graduate Students); European Union's Horizon 2020 Research and Innovation Programme, Grant/Award Number: 720270 (HBP SGA1); Travel support from the Universities Australia/ German Academic Exchange Service (DAAD) Australia-Germany Joint Research Cooperation Scheme grant: "Measuring neural information synthesis and its impairment", Grant/Award Number: PPP Australia Projekt-ID 57216857; Australian Research Council DECRA, Grant/Award Number: DE160100630

## Abstract

The neurophysiological underpinnings of the nonsocial symptoms of autism spectrum disorder (ASD) which include sensory and perceptual atypicalities remain poorly understood. Well-known accounts of less dominant top–down influences and more dominant bottom–up processes compete to explain these characteristics. These accounts have been recently embedded in the popular framework of predictive coding theory. To differentiate between competing accounts, we studied altered information dynamics in ASD by quantifying predictable information in neural signals. Predictable information in neural signals measures the amount of stored information that is used for the next time step of a neural process. Thus, predictable information limits the (prior) information which might be available for other brain areas, for example, to build predictions for upcoming sensory information. We studied predictable information in neural signals based on resting-state magnetoencephalography (MEG) recordings of 19 ASD patients and 19 neurotypical controls aged between 14 and 27 years. Using whole-brain beamformer source analysis, we found reduced predictable information in ASD patients across the whole brain, but in particular in posterior regions of the default mode network. In these regions, epoch-by-epoch predictable information was positively correlated with source power in the alpha and beta frequency range as well as autocorrelation decay time. Predictable information in precuneus and cerebellum was negatively associated with nonsocial symptom severity, indicating a relevance of the analysis of predictable information for clinical research in ASD. Our findings are compatible with the assumption that use or precision of prior knowledge is reduced in ASD patients.

**KEYWORDS**

active information storage, autism spectrum disorder, default mode network, information theory, magnetoencephalography, predictive coding theory, prior knowledge

# 1 | INTRODUCTION

Autism spectrum disorder (ASD) is a developmental disorder with an estimated prevalence of about one in 68 children (Christensen et al., 2016). The disorder is characterized by deficits in social communication together with restricted, repetitive, and stereotyped patterns of behaviors and interests as well as hypo- or hyper-reactivity to sensory input (American Psychiatric Association, 2013). Despite the first descriptions of the disorder by Kanner (1943) and Asperger (1944) dating back more than 70 years, the neurophysiological mechanisms underlying the symptoms of ASD have remained largely unknown. Historically, there have been attempts to elicit specific core underlying cognitive mechanisms. Theories such as the "Theory of Mind" hypothesis (Baron-Cohen, Leslie, & Frith, 1985) assumed to underlie impaired social-cognitive function or executive function impairments (Russell, 1997) and the "weak central coherence" (Happé & Frith, 2006) assumed to underlie stereotyped and repetitive behavior as well as sensory aspects. Examples of sensory and perceptual atypicalities in ASD are decreased susceptibility to visual illusions (Happé, 1996) as well as the superior performance in perceptual tasks requiring a focus on local features compared to global features (Joseph, Keehn, Connolly, Wolfe, & Horowitz, 2009; Plaisted, O'Riordan, & Baron-Cohen, 1998; Shah & Frith, 1983). Recent accounts of ASD further confirm these perceptual characteristics as a key element toward a comprehensive theory of ASD and propose to elucidate the nonsocial symptoms of the disorder within the framework of predictive coding theory (Lawson, Rees, & Friston, 2014; Pellicano & Burr, 2012). Predictive coding theory (Clark, 2013; Friston, 2005, 2010; Kiebel, Daunizeau, & Friston, 2008; Rao & Ballard, 1999) suggests that perception is a process of hierarchical probabilistic inference, in which the brain uses prior knowledge from life-long experience for building internal predictions. These predictions are combined with incoming sensory information to infer the state of the outside world. A mismatch between top–down propagated predictions and sensory evidence results in a bottom–up propagated prediction error (PE). Influence on perception of the PE depends on so-called precision weighting (Friston, 2009; Friston & Kiebel, 2009); that is, the weight that is given to the PE compared to the prediction/prior knowledge.

Predictive coding accounts of perception in ASD can be formalized as changes in information processing in terms of a reduced influence of prior knowledge (Pellicano & Burr, 2012), a relative imbalance of prior knowledge and prediction error (Friston, Lawson, & Frith, 2013; Lawson et al., 2014), or a mere overweighing of prediction error/sensory input (Brock, 2012; Van de Cruys et al., 2014). To differentiate between these accounts, altered information dynamics in ASD may be assessed via the three fundamental component operations of information processing, that is, information storage, transfer, and modification (Gómez et al., 2014; Langton, 1990; Lizier, Prokopenko, & Zomaya, 2012; Wibral et al., 2015). In particular, quantifying information storage in neural signals may be a useful tool for testing the hypothesis of reduced use of prior knowledge in ASD (Gómez et al., 2014) as the use of prior knowledge for predictions requires that (passively) stored information is re-expressed in neural activity (active storage; see Zipser,

Kehoe, Littlewort, & Fuster, 1993 for a distinction between passive and active storage). Information storage in neural processes is mirrored by the fact that information from the past of a neural process predicts a certain fraction of information in the future of this process (Gómez et al., 2014; Wibral, Lizier, Vögler, Priesemann, & Galuske, 2014). This predictable information provides the upper bound of the information potentially becoming useful as predictions for the brain.

In this study, we compared predictable information as measured by the information-theoretic measure active information storage (Lizier et al., 2012) for young patients diagnosed with ASD and neurotypical controls based on neural signals reconstructed from resting-state magnetoencephalography (MEG) recordings.

We hypothesized that predictable information would be reduced in patients with ASD and that reduced predictable information would further be associated with severity in one or more of the symptom domains in ASD.

# 2 | METHODS

## 2.1 | Participants

Nineteen male patients diagnosed with ASD according to ICD-10 (World Health Organization, 1992), that is, autism (F84.0), Asperger Syndrome (F84.5), or atypical autism (F84.1) and nineteen male, neurotypical controls (NTC) aged 14–27 years participated in this study. Exclusion criteria for both groups were an IQ below 70, history of or current diagnosis of schizophrenia or bipolar disorder, current depressive episode, severe anxiety disorder, tic disorder, illegal drug use, and a chronic medical or neurological condition. All participants showed normal or corrected to normal vision. Neurotypical individuals had to score below the clinical cutoff of all first-order scales of the Youth Self Report (YSR; Achenbach & Edelbrock, 1991; Deutsche Child Behavior Checklist, 1998a) or Young Adult Self Report (YASR 18-30; Achenbach, 1990; Deutsche Child Behavior Checklist, 1998b). The ethics committee of the Medical Faculty of the University of Frankfurt approved the experimental study. Participants and/or their parents gave written informed consent before the experiment and received monetary compensation.

ASD patients were recruited through the Department of Child and Adolescent Psychiatry, Psychosomatics and Psychotherapy, University Hospital Frankfurt, Goethe-University and via ASD-related websites. NTC were recruited from local schools and by notices on the university campus.

## 2.2 | Assessment instruments

### 2.2.1 | Assessment instruments across groups

In- and exclusion criteria were assessed using checklists as well as a semi-standardized medical history interview. IQ was measured by the Culture Fair Intelligence Test (CFT 20-R; Weiß, 2006). The German version of the Youth Self Report (YSR) and the German version of the Young Adult Self Report (YASR 18-30) were implemented to describe severity of current psychopathology in both groups.

The socio-economic status (SES) of the respective family was computed based on the mean occupational status of both parents. The occupational status ranged from 1 to 5 (1 = unskilled worker; 5 = highly skilled, leading position). Handedness was assessed according to the Edinburgh Handedness Inventory scale (Oldfield, 1971), in which positive values indicate right handedness and negative values indicate left handedness.

### 2.2.2 | Autism-specific assessment instruments

Patients were diagnosed according to ICD-10 criteria (World Health Organization, 1992), employing a semi-structured clinical interview, the German version of the Autism Diagnostic Observation Schedule (ADOS; Lord et al., 2000; see Rühl, Bölte, Feineis-Matthews, & Poustka, 2004 for the German version), and the Autism Diagnostic Interview–Revised (ADI-R; Rutter, Couteur, & Lord, 2003; see Bölte, Rühl, Schmötzer, & Poustka, 2006 for the German version) administered by experienced clinicians (psychiatrists, clinical psychologists). The ADOS is a direct observation measure, assessing social communication and stereotyped, restricted behaviour within a social interaction situation. The ADI-R is a standardized interview for caregivers of autistic individuals and encompasses the three domains of "social interaction," "communication," and "restrictive, repetitive and stereotyped behaviours and interests." The ADI-R could not be obtained in five of the ASD patients.

### 2.3 | Data acquisition

For each participant, magnetoencephalography (MEG) resting-state recordings were obtained for 5 min each with eyes open (fixating) and eyes closed, respectively. Only analysis of the data obtained from the resting-state recordings with eyes closed will be reported in the main manuscript (for results of the analysis of eyes-open recordings see Supporting Information, Figure 1).

The acquisition of the MEG data was performed in line with the guidelines for "good practice" of MEG recordings (Gross et al., 2012). A whole-head system (Omega 2005; VSM MedTech, Port Coquitlam, BC, Canada) with 275 axial gradiometers was used to record the MEG signals. Signals were recorded continuously at a sampling rate of 1,200 Hz in a synthetic third-order gradiometer configuration and filtered online with fourth-order Butterworth filters with a 300 Hz low pass and a 0.1 Hz high pass (Data Acquisition Software Version 5.4.0, VSM MedTech, BC, Canada). During the complete recording participants' head position relative to the gradiometer array was localized via three head localization coils that were placed on the nasion and 1 cm anterior of the tragus of each ear. To detect artifacts, the horizontal and vertical electrooculogram (EOG) and the electrocardiogram (ECG) were recorded via six electrodes. These were placed distal to the outer canthi of both eyes to record horizontal eye movements, above and below the right eye to record blinks and vertical eye movements and below both collarbones to record the ECG. The impedance of each electrode was kept below 15 kΩ, as measured with an electrode impedance meter (Astro-Med Electrode Impedance Meter, Model F-EZM5, Grass Technologies, Natus Neurology Inc., Warwick RI).

Structural MR images were obtained with a 3 T Siemens Allegra or Trio scanner (Siemens Medical Solutions) using a standard T1 sequence (3D MPRAGE sequence, 176 slices, $1 \times 1 \times 1$ mm voxel size). Before acquisition of the structural images, vitamin E pills were placed at the former positions of the MEG head localization coils to enable co-registration of MEG data and structural MR images.

### 2.4 | MEG data analysis

### 2.4.1 | Preprocessing

MEG data analysis was performed with MATLAB (MATLAB 2012; The MathWorks) and the open source MATLAB toolbox FieldTrip (Oostenveld, Fries, Maris, & Schoffelen, 2011). During preprocessing, the continuous recordings of five minutes were split into data epochs of 1 s each. Line noise was removed using a discrete Fourier transform filter at 50, 100, and 150 Hz. Further, FieldTrip artifact-rejection routines were used to automatically reject epochs containing muscle or sensor jump artifacts. For further cleaning of the data, independent component analysis (ICA; Makeig, Bell, Jung, & Sejnowski, 1996) was performed using the extended infomax (runica) algorithm implemented in fieldtrip/EEGLAB. ICs displaying a strong correlation with EOG and ECG channels were removed from the data. Additionally, data were visually inspected for residual artefacts.

To minimize movement-related inaccuracies, the mean head position in the resting state datasets was calculated for each participant and only epochs in which the head position did not deviate more than 5 mm from the mean head position were considered for analysis.

### 2.4.2 | Source grid creation

To perform MEG source analysis with individual head models, individual source grids were created by transforming the structural MR image for each participant to a T1 MNI template (http://www.fil.ion.ucl.ac.uk/spm). This way an individual transformation matrix was obtained for each participant. Next, the inverse of each participants' transformation matrix was used to warp a regular dipole grid from MNI space to physical (participant) space (based on T1 template, spacing 15 mm, resulting in 478 grid locations inside the brain). Using this approach, every brain area was located at the same grid point for all participants allowing calculation of multi-participant statistics. A realistic single shell forward model (Nolte, 2003) was used to compute the lead-fields for each grid location.

### 2.4.3 | Source time course reconstruction

To enable a whole-brain analysis of active information storage (AIS), we reconstructed the source time courses for all 478 source grid locations inside the brain. Whole-brain source time course reconstruction was performed using a time-domain beamformer filter (linear constrained minimum variance, LCMV; Van Veen, Van Drongelen, Yuchtman, & Suzuki, 1997) applied on MEG sensor data filtered broadly with 8 Hz high pass and 150 Hz low pass. For each of the 478 source grid location three orthogonal filters in x, y, and z direction were computed and the sensor data were projected through the LCMV filters. From the resulting three time courses per location via singular value

decomposition, the time course in direction of the dominant dipole orientation was obtained and used for calculation of AIS.

### 2.4.4 | Analysis of active information storage (AIS)

AIS describes how much of the information in the next time step of a process is predictable from its immediate past embedded (time-series) state (Lizier et al., 2012). High AIS values indicate that a signal is both rich in information and predictable at the same time. Detailed definition of AIS is given in Lizier et al. (2012) (methods part) and Wibral et al. (2014) (see also Gómez et al., 2014 and Brodski-Guerniero et al., 2017 for applications on MEG data).

To determine the history dimension and optimal embedding delay parameter for AIS computation, the Ragwitz criterion (Ragwitz & Kantz, 2002) as implemented in the TRENTOOL toolbox (Lindner, Vicente, Priesemann, & Wibral, 2011) was used for each participant and each of the source locations separately. As differences in history dimension may induce a bias on the estimated values, we chose the history dimension of 6 over all participants and source locations for computation of AIS. This means that 6 samples were chosen, spaced at an embedding delay interval that was individually determined per participant based on that participant's signal autocorrelation decay time and the optimization via the Ragwitz criterion (see Supporting Information, Table 1 for the distribution of embedding delays across participants). No significant correlation between embedding delay and mean AIS was found (Spearman's rho = −.17, $p = .29$; Pearson's $r = −.22$, $p = .2$, see Supporting Information, Figure 2). This indicates that the resulting AIS values are not sensitive to the choice of the embedding delay. Also no significant difference in embedding delay between the ASD and NTC group was observed (Wilcoxon ranked sum test $p = .14$).

AIS was computed with 4 nearest neighbors (recommended by Kraskov, Stögbauer, & Grassberger, 2004) in the joint embedding space using the Kraskov–Stoegbauer–Grassberger estimator (Kraskov et al., 2004) (algorithm 1), as implemented in the open source Java Information Dynamics Toolkit (Lizier, 2014). Data points from all epochs and time points were accumulated (for each source location and participant) for the computation of distributions underlying the AIS analysis. As a different number of data points may induce a bias in the estimation, AIS was computed on embedded data only up to the minimal number of data points over participants (number of data points entering the analysis: 149987).

Each sample from an epoch and a time point was assigned a local AIS (LAIS) value based on the overall distribution (assuming stationarity, see Lizier et al., 2012). Later the LAIS estimates for individual data points were averaged across time for each epoch of one sec to obtain the AIS value for that epoch, source location, and participant.

### 2.4.5 | Statistical analysis on AIS

For investigation of the mean difference in AIS between ASD patients and NTC, for each participant, the AIS values were also averaged over all epochs and over all 478 source locations and a Wilcoxon rank sum test was performed to test for AIS differences between groups. To examine a potential correlation of AIS and age, Pearson's $r$ and Spearman's rho were calculated for each group separately.

For finding the specific source locations at which AIS values differed between groups, an independent samples permutation $t$ test was performed across all potential source locations over the whole brain. To account for multiple comparisons across the 478 source locations, a cluster-based correction method (Maris & Oostenveld, 2007) was used. Clusters were defined as adjacent grid points whose $t$ values exceeded a critical threshold corresponding to an uncorrected alpha level of 0.05. For these clusters we defined cluster values as the sum of $t$ values in a particular cluster. Cluster values were tested against the distribution of cluster values obtained from 5,000 permuted data sets. Significance was assessed based on an alpha value of 0.05. For the significant clusters, the brain areas showing (local) peaks in the $t$ map were reported. For these locations, we also calculated Spearman's and Pearson's correlations of AIS with age.

To assess the relationship of AIS values and ADI-R ratings of symptom severity (Bölte et al., 2006), linear regression analysis with AIS (mean over epochs) as response variable and the ADI-R algorithm scores as the predictor variable were calculated for all 478 brain locations. To account for multiple comparisons across brain locations, a cluster-based correction method was performed on the $t$ values of the beta coefficients ($t$ = beta/standard error). Cluster significance was assessed in the same way as for the independent sample $t$ statistic described above (5,000 permutations, alpha 0.05). Linear regression analysis was performed separately for each of the three ADI-R domains "communication" (ADI-com), "social interactions" (ADI-soc), and "restrictive, repetitive and stereotyped behaviours and interests" (ADI-rit). Please note that ADI-R scores were available for 14 of the 19 ASD patients only, and thus this part of the analysis is based on a smaller sample size than the rest.

### 2.4.6 | Correlation analysis of AIS and beamformer reconstructed source power/autocorrelation decay time

We further investigated the relationship of AIS and spectral power in individual epochs using Spearman's correlations. The frequency bands for correlation analysis were determined based on the averaged and normalized spectrum (by multiplication with frequency to account for the 1/f shape of the non-normalized spectrum) of the peak sources showing significant differences in AIS between groups. The spectrum was calculated from the reconstructed source time courses using a multitaper approach (Percival & Walden, 1993) with 2 Slepian tapers (Slepian, 1978) for a frequency interval from 8 to 150 Hz in 2 Hz steps. The averaged spectrum over sources, participants and epochs revealed three frequency bands: 8–14 Hz (alpha); 14–36 Hz (beta); and 36–150 Hz (gamma). Epoch-by-epoch power in these frequency bands was used for calculation of the Spearman's correlation with epoch-by-epoch AIS. For each participant Spearman's rho was computed for correlation of the epoch-by-epoch power (median over coefficients in each of the predefined frequency bands) with the epoch-by-epoch AIS.

Correlation analysis was additionally performed for epoch-by-epoch AIS and a more traditional measure of time series analysis, autocorrelation decay time (ACT). ACT was computed as the lag at which the autocorrelation function for each epoch of the reconstructed source time course decayed below the fraction of 1/$e$ of its center peak.

To test the significance of the correlation of epoch-by-epoch AIS and epoch-by-epoch power or ACT, for each participant the epochs were randomly permuted 5,000 times and correlation was re-calculated for the permuted data sets. For each participant, an original correlation value more extreme than 99.9998% (threshold Bonferroni adjusted for the $38 \times 3 \times 3$ multiple comparisons) of the correlation values obtained for the permuted data sets was considered to be significant. At the second level, a binomial test was used to assess whether the number of participants showing significant correlations could be explained by chance. The median correlation values over participants and their significance based on the binomial test are reported.

### 2.4.7 | Complexity analysis

As the AIS in a signal is a function of the average information contained in that signal (i.e., entropy; Shannon, 2001) as well as how this is self-related over time lags, we also quantified the differential entropy (Cover & Thomas, 2012) at the brain locations showing significantly decreased AIS for patients.

Thereby we aimed to investigate whether decreased AIS in ASD was also associated with decreased (differential) entropy values. Differential entropy was calculated from the continuous signals using the Kozachenko–Leonenko estimator (Kozachenko & Leonenko, 1987) as implemented in the Java Information Dynamic Toolkit (Lizier, 2014). To avoid a bias for the estimation of entropy based on a differential amount of epochs, the minimal number of 127 epochs was used for entropy estimation of all participants. A Wilcoxon rank sum test was used to access the differences in differential entropy between the ASD patients and the NTC group.

### 2.4.8 | Statistical analysis using Bayesian statistics

As nonsignificant effects were found for the difference in entropies between groups as well as for the correlation of AIS values and age, we additionally report Bayes factors (BF; Jeffreys, 1998) to clarify these findings. BFs allow direct quantification of the weight of evidence in favor of the null or the alternative hypothesis (Dienes, 2014)—a measure that cannot be obtained just by failing to reject the null hypothesis in a frequentist approach. BFs were computed with the BayesFactor package (Morey, Rouder, Jamil, & Morey, 2015) in R (R Core Team, 2016). Default (medium width) prior settings for linear regression were used (Jeffrey–Zellner–Siow mixture of g-priors; Rouder & Morey, 2012; see also Liang, Paulo, Molina, Clyde, & Berger, 2008, Section 2.1), not favoring the null or alternative hypothesis in advance. For equal priors for the alternative and the null hypothesis a BF of, for example, 3 indicates that the posterior odds are 3:1 in favor of the alternative hypothesis, that is, that the alternative hypothesis is three times more probable than the null hypothesis given the data and the prior probabilities of both hypotheses.

Three types of BF comparisons were performed in this study:

1. For average AIS (over the whole brain) as a response variable, we compared BFs for a linear regression with age as a predictor variable, with a linear regression with group (i.e., ASD or NTC) as a predictor variable.

2. For AIS in difference areas (mean over the brain areas showing a significant difference in AIS between the NTC and the ASD group) as a response variable, we compared BFs for a linear regression with age and group as predictor variables with a linear regression including only group as a predictor variable. Note that here the factor group was included in the "null model" as the brain areas were pre-selected based on a group comparison in the independent samples $t$ test.

3. For differential entropy as the response variable, we compared BFs for a linear regression with group as predictor variable with a linear regression "null model" including the intercept only.

### 2.4.9 | Control analyses

Owing to the finding of a strong positive correlation of epoch-by-epoch AIS and epoch-by-epoch alpha power as well as ACT, we conducted several control analyses to demonstrate that the AIS measure provides additional information which is not provided by these two more traditional measures.

First, we calculated a correlation of the $t$-value map based on the AIS contrast and the $t$-value map based on the alpha power or ACT contrast (see also Brodski-Guerniero et al., 2017 for a similar analysis). For all $t$-value maps, the independent samples $t$-metric ASD versus NTC was computed for all 478 source locations within the brain on the respective values (AIS, ACT, alpha power) averaged over all epochs.

Then, we repeated the statistical group analysis performed for AIS also for alpha power and ACT:

For investigation of the mean difference between ASD patients and NTC for each participant, alpha power/ACT values were averaged over all epochs and over all 478 source locations and a Wilcoxon rank sum test was performed to test for differences between groups. To find the specific source locations at which alpha power/ACT values differed between groups, an independent samples permutation $t$ test was performed across all potential source locations over the whole brain. To account for multiple comparisons across the 478 source locations, a cluster-based correction method (Maris & Oostenveld, 2007) was used. Clusters were defined as adjacent grid points whose $t$ values exceeded a critical threshold corresponding to an uncorrected alpha level of 0.05. Cluster significance was assessed in the same way as described for AIS statistical analysis.

Finally, we also conducted BF analysis on mean values (averaged over all 478 source locations) to exclude the possibility that alpha power and ACT might be more strongly associated with group differences than AIS. To this end, we compared BFs using a linear regression with AIS, alpha power or ACT as the response variable and group as predictor variable with a linear regression "null model" including the intercept only.

## 3 | RESULTS

### 3.1 | Group characteristics

Nineteen patients diagnoses with ASD and 19 neurotypical controls (NTC) participated in the experiment. The patients were diagnosed

**TABLE 1** Summary of group characteristics

| | ASD (mean ± SD) | NTC (mean ± SD) | Statistics (Wilcoxon rank sum test) |
|---|---|---|---|
| IQ | 109.4 (±16.4) | 109.6 (±18.6) | $p = .861$ |
| Age | 18.7 years (±3.4) | 21.6 years (±3.8) | $p = .041$ |
| Handedness | 69.5 (±47.5) | 65.5 (±51.6) | $p = .388$ |
| SES | 3.3 (±1.03) | 3.9 (±0.79) | $p = .097$ |
| Y(A)SR SR | 61.6 (±11.9) | 51.9 (±3.3) | $p = .006$ |
| Y(A)SR KB | 57.3 (±10.3) | 52.6 (±4.3) | $p = .169$ |
| Y(A)SR ADP | 57.4 (±9.5) | 51.5 (±2.5) | $p = .036$ |
| Y(A)SR SP | 59.7 (±13.6) | 52.8 (±6.2) | $p = .06$ |
| Y(A)SR SZ | 60.3 (±10.9) | 50.4 (±1.8) | $p = .0005$ |
| Y(A)SR AP | 59.6 (±10.7) | 52.3 (±3.4) | $p = .013$ |
| Y(A)SR AV | 53.6 (±5.8) | 51.7 (±3.5) | $p = .153$ |
| Y(A)SR DV | 53.3 (±4.7) | 52.4 (±3.9) | $p = .577$ |
| Y(A)SR INT | 57.1 (±13.1) | 47.2 (±6.5) | $p = .019$ |
| Y(A)SR EXT | 49.8 (±7.7) | 45.7 (±8.5) | $p = .156$ |

*Note.* Abbreviations: ADP = anxious/depressed; AP = attention problems; AV = aggressive behavior; DV = delinquent behavior; EXT = externalizing; INT = internalizing; KB = somatic complaints; SES = socio-economic status; SP = social problems; SR = withdrawn; SZ = thought problems.

with either high functioning autism ($n = 12$), Asperger ($n = 6$), or atypical autism ($n = 1$). Eight of the participants in the ASD group received medication (2× Risperidon, 3× psychostimulant, 2× SSRI, 1× Risperidon, psychostimulant, and SSRI). Main characteristics for both groups are summarized in Table 1.

NTC and ASD were well matched with regard to IQ ($p = .861$), handedness ($p = .388$), and socio-economic status (SES) ($p = .097$). The ASD group was younger than the NTC group ($p = .041$), so age was controlled for during analysis. As expected from the in- and exclusion criteria, several first- and second-order scales of the Y(A)SR ($t$ values) differed between groups.

## 3.2 | Analysis of average predictable information

Comparison of average predictable information as measured by active information storage (AIS) between the ASD and NTC group revealed a significantly reduced mean AIS for the ASD group (Wilcoxon rank sum test, $p = .031$; median ± SD: ASD 2.02 ± 0.08; NTC 2.08 ± 0.06; Figure 1).

To exclude the possibility that group differences in average predictable information were related to age differences between participants, a correlation analysis between AIS and age was performed for each group. No significant correlation with age was found for any of the groups (ASD Spearman's correlation rho = .36, $p = .135$; Pearson's correlation $r = .19$, $p = .428$; $n = 19$; NTC Spearman's correlation rho = .06, $p = .815$; Pearson's correlation $r = .15$, $p = .530$, $n = 19$). To further clarify these nonsignificant results, we also calculated the ratio of Bayes Factors for a linear regression with average AIS as a response variable and group (i.e., ASD or NTC) as a predictor variable and a linear

regression with the same response variable and age as a predictor variable. The resulting Bayes Factor ratio of 3.15 indicated that the observed average AIS values were over three times more likely to occur when group was considered the predictor than when age was considered the predictor. In other words, the calculated Bayes Factor ratio indicated that group was a better predictor on average AIS than age. Thus, it is unlikely that the observed group differences on average AIS were based on age differences only.
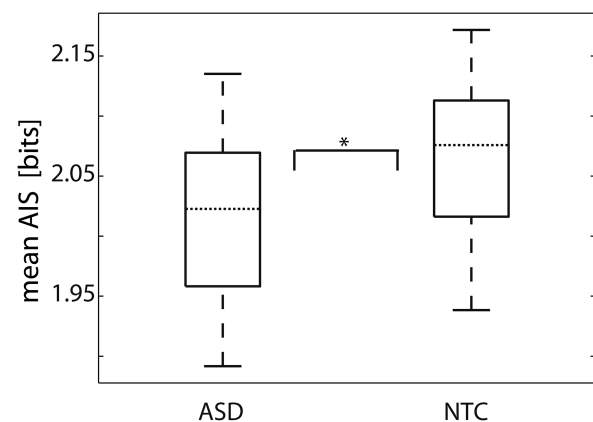


**FIGURE 1** Comparison of average AIS between groups. Each boxplot shows the distribution of averaged AIS values for all participants within the ASD or NTC group, respectively ($n$ ASD = 19, $n$ NTC = 19). These values have been obtained by averaging AIS for all 478 sources inside the brain for each participant. Horizontal dotted lines mark the median of each group. The asterisk indicates a significant difference in average AIS between groups (Wilcoxon rank sum test $p = .03$)
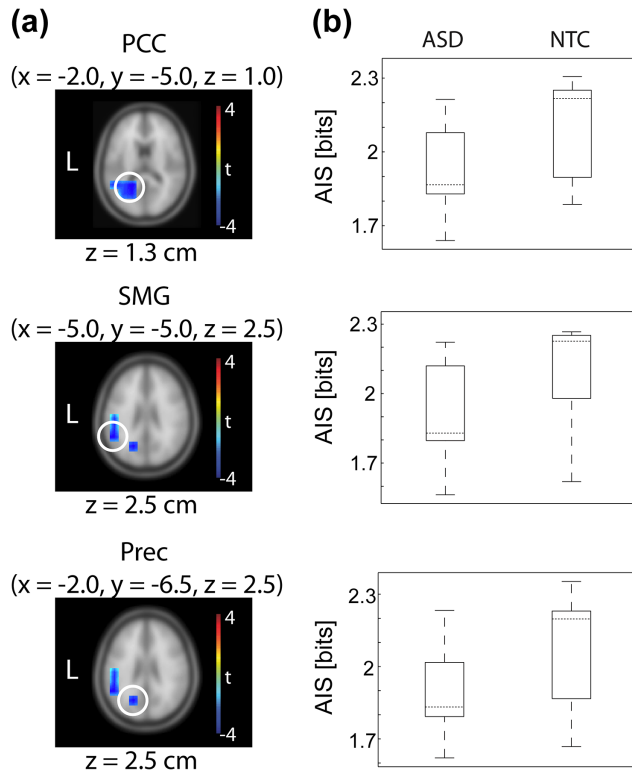
## (a)



**PCC**
(x = -2.0, y = -5.0, z = 1.0)

z = 1.3 cm

**SMG**
(x = -5.0, y = -5.0, z = 2.5)

z = 2.5 cm

**Prec**
(x = -2.0, y = -6.5, z = 2.5)

z = 2.5 cm

## (b)

**FIGURE 2** Statistical comparison of AIS between groups at the MEG source level. *Left*: Results of whole-brain independent samples permutation *t*-metric contrasting the ASD and NTC group (*n* ASD = 19, *n* NTC = 19, *t* values masked by *p* < .05, cluster correction). Peak brain locations are highlighted with white circles. For each brain location, MNI coordinates are shown at the top. An exemplary brain slice is shown for each brain location; *z* values are displayed below each brain slice. *Right*: Illustration of the distribution of AIS values for each brain location and for the ASD and NTC group, respectively. Dotted horizontal lines mark the median of each group. PCC = posterior cingulate cortex; SMG = supramarginal gyrus; Prec = precuneus [Color figure can be viewed at wileyonlinelibrary.com]

### 3.3 | Whole-brain analysis of predictable information

Spatially resolved comparison of AIS between the ASD and NTC group at the MEG source level revealed a significant group difference in posterior cingulate cortex (PCC), supramarginal gyrus (SMG), and precuneus (Prec) (Figure 2a). At these areas, AIS was significantly reduced for ASD compared to NTC (Figure 2b).

To exclude age-related effects, again correlations with age as well as Bayes Factor comparisons were performed. No significant correlation was found for AIS (averaged over the three sources) and age for any of the groups (ASD Spearman's correlation rho = −.04, *p* = .873; Pearson's correlation *r* = .312, *p* = .19; *n* = 19; NTC Spearman's correlation rho = .16, *p* = .499; Pearson's correlation *r* = .02, *p* = .927, *n* = 19). Further, Bayes Factors were computed based on a linear regression with AIS as response variable and group as a predictor variable, and a linear regression with the same response variable and group as well as age as predictors. Please note that here the factor group was included in both models, as the brain areas had been pre-selected based on the group comparison. The resulting Bayes Factor ratio of

3.25 indicated that the observed AIS values were over than three times more likely to occur with group as a predictor than with group as well as age as predictors. This means that a model with group as the only predictor predicted the AIS values better than when age was included as an additional predictor. Thus, similar to the global AIS effect, group differences in AIS at the identified specific sources were not likely to be driven by differential age.

### 3.4 | Complexity analysis

To study whether lower AIS in ASD might be associated with decreased signal complexity, we also computed a measure of entropy in PCC, SMG, and Prec. None of these areas showed significant differences in entropy between groups (Wilcoxon rank sum test, PCC *p* = .599, SMG *p* = .350, Prec *p* = .884, Figure 3). Additionally, a Bayes factor of 0.34 for a linear regression with entropy (averaged over the three brain areas) as response variable and group as predictor variable indicated that the present entropy values were 2.94 times more likely to be observed in case of the validity of the null hypothesis, that is, when group is not a proper predictor for entropy. This suggests that there was no difference in entropy between groups and thus differences in AIS for these source locations were not likely to be based on differences in signal complexity in these areas.

### 3.5 | Correlation of predictable information and power/autocorrelation decay time in individual epochs

To study the relation of AIS and more traditional analysis measures like spectral power and autocorrelation decay time (ACT) over individual epochs in PCC, SMG, and Prec, we correlated single epoch AIS values with the power in different frequency bands as well as with ACT during the same epochs (Table 2). Correlation analysis revealed a strong positive correlation with power in the alpha band, a moderate positive
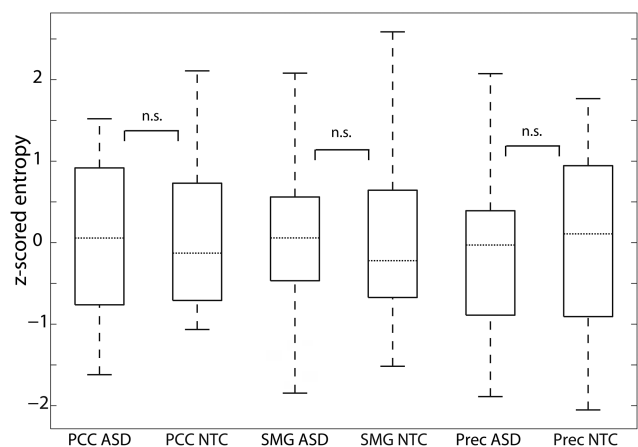


**FIGURE 3** Post-hoc complexity analysis. Boxplots illustrate the distribution of entropy values across participants. Entropies are displayed as *z* scores across all estimates for both groups. Dotted horizontal lines mark the median of each group. n. s. = not significant based on Wilcoxon rank sum test. PCC = posterior cingulate cortex; SMG = supramarginal gyrus; Prec = Precuneus

**TABLE 2** Correlation of epoch-by-epoch AIS values and power/ACT in PCC, SMG, and Prec

|  | PCC | SMG | Prec |
|---|---|---|---|
| 8–14 Hz (alpha) | rho = .69* | rho = .71* | rho = .74* |
| 14–36 Hz (beta) | rho = .35* | rho = .35* | rho = .40* |
| 36–150 Hz (gamma) | rho = −.13 | rho = −.13 | rho = −.12 |
| ACT (autocorrelation decay time) | rho = .89* | rho = .46* | rho = .67* |

*Significant correlation, based on binomial test.

correlation with power in the beta band as well as a strong positive correlation with ACT.

## 3.6 | Comparison of AIS analysis with more traditional analysis methods

While we found a strong positive correlation of epoch-by-epoch alpha power/ACT and predictable information, the contrast map (t values for all source grid points obtained from independent sample t metric; ASD vs NTC) based on the mean alpha power over epochs did not correlate with the epoch-mean AIS contrast map (Spearman's rho = .02, p = .66; Pearson's r = .01, p = .88; Figure 4). The corresponding contrast map based on mean ACT, showed a (weak) negative correlation with the mean AIS contrast map (Spearman's rho = −.29, p < .01, Pearson's r = −.3, p < .01; Figure 4).

We also repeated the group comparison which we performed for AIS for alpha power and ACT, following the same pipeline and statistical thresholds as for AIS: For the spatial-average values (averaged over all sources over the whole brain), no significant differences between the ASD and NTC group were found neither for alpha power (median alpha ASD: $9.4 \times 10^{-8}$; median alpha NTC: $7.5 \times 10^{-8}$, Wilcoxon ranked sum test, p = .21), nor ACT (median ACT ASD: 8.1, median ACT NTC: 7.3, Wilcoxon ranked sum test, p = .1). In addition, for the whole-brain contrast of ASD and NTC, no significant clusters were found for the independent samples permutation t test, neither for alpha power nor ACT (cluster correction, p > .07).

Last, Bayes factor analysis revealed a Bayes factor of 3.2 for a linear regression with (averaged) AIS as a response variable and group as predictor variable, compared to a null model, indicating that group properly predicts the AIS values. For a linear regression with group as a predictor variable and (averaged) alpha power as a response variable we found a Bayes factor of 0.39 and for (averaged) ACT as response variable we found a Bayes factor of 0.92, indicating that group is less likely to be a proper predictor for these two measures. In other words, group membership is most cleanly expressed in AIS values.

The closer link between mean AIS and group, compared to mean ACT and group, but also the strong correlation of ACT and AIS at the single epoch level may be explained by the fact that ACT is a linear measure of how long information is maintained in a signal, while AIS is a measure of how much information is maintained in a signal for the history length considered (which was related to the ACT here). Thus,
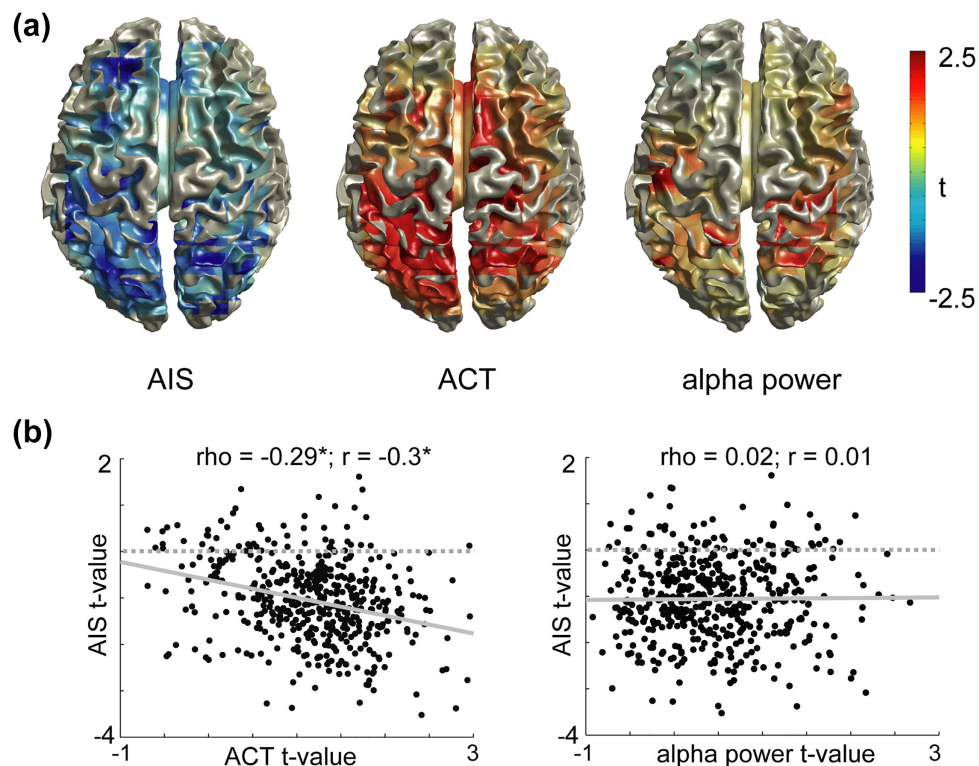


**FIGURE 4** Correlation of AIS contrast maps and ACT/alpha source power contrast maps. (a) Illustration of the t value maps of the independent samples t-metric for the ASD versus NTC contrast (n = 38, no correction) on the cortical surface. (b) Scatter plots of the relationship of the ACT/alpha power contrast and the AIS contrast. Each dot represents a source location within the brain. Spearman and Pearson correlation values on top of each plot (n = 478). Linear regression lines are included in gray (solid) [Color figure can be viewed at wileyonlinelibrary.com]
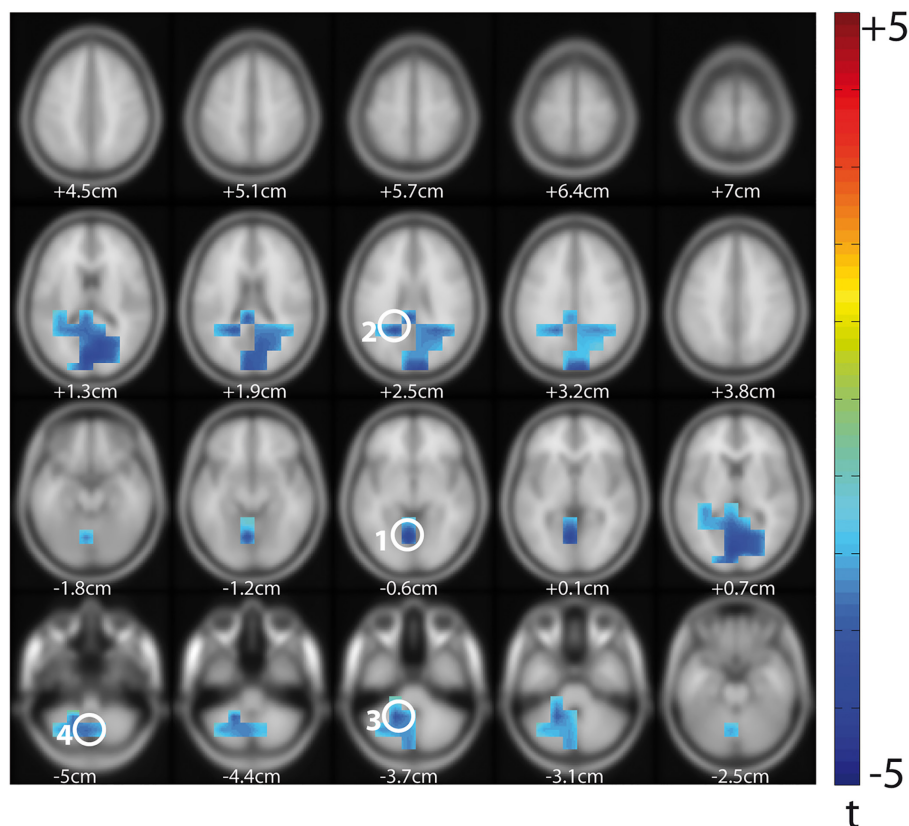
**FIGURE 5** Linear regression analysis of AIS and ADI-R scores. Results of linear (permutation) regression with ADI-R rit algorithm scores as predictor variable and AIS as response variable (ASD only, $n = 14$, $t$ values masked by $p < .05$, cluster correction). Z values are shown below each brain slice. Peak voxels are highlighted with white circles and numbers; corresponding MNI coordinates and labels are given in Table 3 [Color figure can be viewed at wileyonlinelibrary.com]

ACT is a lossy nonlinear transform of the more informative AIS measure.

Summing up these findings, while single epoch AIS values were strongly linked to single epoch alpha power and single epoch ACT, analysis of mean AIS showed that this novel measure provides additional information not directly provided by a simple spectral analysis or an analysis of ACT (Brodski-Guerniero et al., 2017; Gómez et al., 2014; Wollstadt et al., 2017).

## 3.7 | Correlation of predictable information and ADI-R scores

To further assess whether predictable information relates to autistic traits, we performed a whole-brain linear regression analysis of AIS and the three ADI-R algorithm scores for the ASD group ($n = 14$ as ADI-R scores were not available for all of the patients). Regression analysis was performed separately for the three domains: communication (ADI-R com), social interactions (ADI-R soc), and restrictive, repetitive and stereotyped behaviors and interests (ADI-R rit). There was a significant cluster for the regression of AIS and ADI-R rit (Figure 5). This cluster encompassed four peak areas, including sources in the cerebellum and the precuneus. The source in precuneus was located slightly more anterior compared to the precuneus area found in the group comparison of AIS (see MNI coordinates in Table 3). All of the brain areas in

the significant cluster showed a negative $t$ value, indicating a negative relationship of AIS and ADI-R rit. In other words, lower AIS in these areas was associated with higher ADI-R rit scores, that is, a higher degree of impairment in this domain. No significant clusters were found for the regression of AIS and ADI-R com or ADI-R soc.

## 4 | DISCUSSION

Inspired by the suggestion of impaired predictive coding mechanisms in ASD, we tested the hypothesis that predictable information in neural signals is reduced in ASD patients. In line with this hypothesis, we found average predictable information to be reduced in individuals with ASD compared to neurotypical controls (NTC) during resting-state

**TABLE 3** Peak voxels for the significant cluster in the regression analysis of AIS and ADI-R rit (Figure 5)

| No | MNI coordinates | Label |
|---|---|---|
| 1 | $x = -5$, $y = -65$, $z = -5$ | Left lingual gyrus/cerebellum (culmen) |
| 2 | $x = -20$, $y = -50$, $z = 25$ | Left precuneus |
| 3 | $x = -20$, $y = -50$, $z = -35$ | Left cerebellum |
| 4 | $x = -5$, $y = -65$, $z = -50$ | Left cerebellum (lobule VIII) |

magnetoencephaography (MEG) recordings. In addition to the reduction of average predictable information in ASD, we found specific reductions of predictable information in posterior cingulate cortex (PCC), supramarginal gyrus (SMG), and precuneus (Prec). Importantly, none of the group differences in predictable information could be accounted for by differences in age between the participants or by differences in signal complexity (entropy) between groups. In addition, predictable information in ASD patients showed a negative relationship with symptom severity in the domain of restricted, repetitive, and stereotyped behaviors and interests (ADI-R rit) in several brain areas including the cerebellum, suggesting a potential clinical relevance of predictable information in ASD research.

In the following, we will relate our results to previous findings and predictive coding accounts of perception in ASD.

## 4.1 | Average predictable information is reduced in ASD

Our finding of reduced average predictable information in ASD is in line with a recent report by Gómez et al. (2014). Gomez et al. studied predictable information using the AIS measure (Lizier et al., 2012) in ASD patients and NTC in the pre-stimulus interval of a face detection task. In all but one of the 12 studied brain regions they found at least a tendency toward a reduction of AIS in ASD. This study confirms this general finding of reduced predictable information in ASD—while overcoming several shortcomings of the predecessor study: First, the present larger sample of 38 (19 patients, 19 controls) improved statistical power in contrast to the small sample size of 22 (10 patients, 12 controls) in the previous study (Gómez et al., 2014). Second, in contrast to the region-of-interest approach by Gomez et al., applying a whole-brain approach allowed to study the (average) differences in AIS between groups based on a large amount of sources (∼500 inside the brain) covering all potential brain areas. Thus, the present study demonstrated that overall AIS is reduced in patients with ASD.

## 4.2 | Predictable information at PCC, SMG, and Prec is reduced in ASD

Whole-brain analysis of AIS additionally enabled to determine the brain areas at which predictable information was particularly reduced for ASD patients. This was the case for PCC, SMG, and Prec. These three brain areas belong to the default mode network (DMN; Buckner, Andrews-Hanna, & Schacter, 2008; Mason et al., 2007; Raichle, 2015), which is known to be engaged during passive (internally focused) tasks or epochs—corresponding to the resting-state design of this study. Atypicalities in the DMN for ASD patients have been reported as reduced activation of the DMN nodes (Kennedy, Redcay, & Courchesne, 2006) or as altered, mainly diminished connectivity between the nodes (Cherkassky, Kana, Keller, & Just, 2006; Washington et al., 2014; Weng et al., 2010). However, hyperconnectivity of posterior nodes has also been reported, namely to medial and anterior temporal lobe regions (Lynch et al., 2013; Monk et al., 2009). Further, ASD atypicalties in the DMN may also be related to anatomical differences such as a relative increase of gray matter volume in several brain areas including the PCC in ASD patients (Waiter et al., 2004). Interestingly, internal thoughts which mainly involve activity in the DMN (Buckner et al., 2008) are also reported to differ considerably between NTC and ASD patients (Hurlburt, Happe, & Frith, 1994). Extending these previous findings of ASD-related atypicalities in the DMN, our results show that for ASD patients also the amount of predictable information is particularly reduced in posterior nodes of the DMN during resting state periods. It should be noted that reductions of predictable information in ASD may appear in brain regions other than the DMN, when the task requires specific predictions (Gómez et al., 2014).

## 4.3 | Complexity is not reduced in PCC, SMG, and Prec

Noteworthy, decreased predictable information within the DMN as assessed by AIS was not associated with decreased signal complexity in these areas. This is of importance as the AIS measure quantifies both the complexity and predictability of neural processes. High AIS values are observed for predictable signals, but this increases with the richness of cortical dynamics that are self-predictable. In particular, complexity, which can be measured as signal entropy (i.e., average information content), contributes to AIS.

Thus, in principle, reduced AIS in ASD patients could also have resulted from a reduced signal complexity. Indeed, reduced EEG signal complexity has been observed during a visual matching task for ASD patients (Catarino, Churches, Baron-Cohen, Andrade, & Ring, 2011) as well as during resting-state recordings for children with a high risk of developing ASD (Bosl, Tierney, Tager-Flusberg, & Nelson, 2011). However, these previous findings were not replicated in our study using differential entropy as a measure of complexity. Our Bayesian analysis favored the hypothesis that there is no difference in entropy and thus complexity between ASD patients and NTC for the three DMN areas. Note that at the descriptive level, even the sign of the marginal differences in entropy between groups was not the same over brain areas. These findings suggest that neural signals in the DMN for patients and controls were equally rich in cortical dynamics; however, they were structured in a less predictable manner for the ASD group. In the following, we relate our findings to predictive coding accounts of ASD.

## 4.4 | Reduced predictable information in the light of predictive coding accounts of ASD

Recently it has been argued that the DMN may play a key role in predictive coding by acting as a top level of the predictive hierarchy, being responsible for initiating predictions that cascade down to categorize sensory input and drive motor activity (Barrett, 2017; Barrett & Satpute, 2013). This postulated high impact of the DMN in predictive processing is compatible with the key functions associated with the DMN like episodic memory retrieval (posterior parietal and PCC regions), future planning, self-referential thoughts (dorsomedial prefrontal cortex; PFC), and integrating sensory and interoceptive signals (ventromedial PFC; Buckner et al., 2008; Raichle, 2015; Whitfield-

Gabrieli & Ford, 2012). In particular, the posterior regions of the DMN like the Prec and PCC have been linked to memory-related processing, that is, retrieving information from memory and anticipating the future (Bar, 2007; Buckner et al., 2008; Wagner, Shannon, Kahn, & Buckner, 2005). Bar (2007) linked the DMN even more directly to the continuous generation of (memory-based) predictions in the brain. Extending this line of thought, Fiser, Berkes, Orbán, and Lengyel (2010) have suggested that spontaneous brain activity (as for instance within the DMN during resting state recordings) reflects the historically informed prior beliefs about the world (Sadaghiani, Hesselmann, Friston, & Kleinschmidt, 2010). Based on these suggestions our findings of decreased predictable information in ASD within the DMN seamlessly fit into the account of reduced use of prior knowledge or "weaker" prior beliefs in ASD (Pellicano & Burr, 2012). As the neural signals in the DMN for ASD patients were structured in a less predictable manner during rest, we might speculate that this reflects the impairment of ASD patients to represent the high-level regularities of the environment in their spontaneous activity.

The fact that this effect was found at posterior nodes of the DMN could indicate that there is a deficit in retrieving information from memory (Raichle, 2015) to generate appropriate predictions. One hypothetical mechanism for this deficit could be related to the previously reported functional hyperconnectivity between the PCC and medial and anterior temporal lobe regions (Lynch et al., 2013): if too much or nonspecific information is retrieved more or less at random during rest, it may impair the ability to generate stable predictions that would show as AIS.

Aside from this speculation, our data strongly suggest that the brain areas receiving the information from the DMN will need to deal with information that is less predictable. This may result in difficulties to learn (or change) new predictive models, leading to even more unreliable representations of the world. Reduced reliability or precision of prior knowledge for the formation of top–down propagated predictions may further result in an imbalance of bottom–up and top–down influences in ASD (Friston et al., 2013; Lawson et al., 2014). A relative increase of the influence of bottom–up propagated prediction error may lead to the feeling of being overwhelmed by sensory information (Grandin,1992), as weak or imprecise predictions will be less efficient in explaining away sensory inputs, thus leaving more feed-forward sensory information to be processed by relatively limited central resources.

While our results are fully compatible with predictive coding accounts of perception in ASD, which highlight the reduced use or (relative) precision of priors (Friston et al., 2013; Lawson et al., 2014; Pellicano & Burr, 2012), they are not easily explained by accounts of merely increased bottom–up precision in ASD (Brock, 2012; Van de Cruys et al., 2014). This is because increased bottom–up precision should not be associated with decreased predictable information.

Furthermore, our finding of the strong association of epoch-by-epoch predictable information in resting state recordings and neural activity in low frequencies adds support to the hypothesis that low frequencies are the carrier of top–down propagated information within

the predictive coding framework (Bastos et al., 2012; see, e.g., Brodski-Guerniero et al., 2017 for empirical evidence).

## 4.5 | Predictable information in ASD is associated with symptom severity in the ADI-R rit domain

Studying predictable information in ASD may not only help to distinguish between competing theoretical accounts but may also have a potential clinical relevance. This is supported by the finding of a significant negative relationship between predictable information and the symptom severity in the ADI-R rit domain. The ADI-R rit domain captures mainly stereotypical motor behaviors like hand flapping as well as the insistence on sameness and routines. Thus, in contrast to deficits in social interactions (ADI-R soc) and communication (ADI-R com), the ADI-R rit domain of ASD symptoms is maybe most closely related to perceptual atypicalities and also predictive coding mechanisms in ASD. In fact, the behavioral abnormalities captured in this domain might represent techniques to control the exaggerated prediction error resulting from the imbalance of top-down and bottom–up information flow (Friston et al., 2013; Lawson et al., 2014) and reduce the anxiety associated with the inability to predict upcoming events (Sinha, 2002).

The significant cluster for the regression of ADI-R rit scores and AIS included prominent peaks in the cerebellum—a brain area in which anatomical abnormalities in ASD (e.g., decreased number of Purkinje cells) have been observed most consistently (Brambilla et al., 2003; see also Fatemi et al., 2012 for a review). Even more closely related to our findings, a significant negative correlation between rates of repetitive behavior and area measures of cerebellar vermis lobules VI–VII has been previously reported (Pierce & Courchesne, 2001). Based on this finding we might speculate that anatomical abnormalities in the cerebellum would also show a correlation with the AIS measure. However, this remains to be tested in future investigations.

## 5 | CONCLUSION

Resting-state neural activity in patients with ASD shows less predictable information compared to controls. This is particularly the case for posterior regions of the default mode network. Further, in cerebellum and precuneus, signal predictability is negatively associated with symptom severity in the domain of restricted and repetitive behaviors. Thus, AIS appears to be a sensitive measure describing differences in neural information processing between patients with ASD and neurotypical controls. Extensive comparisons to more traditional descriptors of neural dynamics such as spectral power and autocorrelation times suggest that AIS uncovers additional group differences not seen in these other measures. Last, our findings of reduced predictable information in patients with ASD replicate at the whole-brain level our earlier results based on a more limited region-of-interest analysis.

## ORCID

*Alla Brodski-Guerniero* http://orcid.org/0000-0002-5852-4750

*Fernando Ferreira-Santos* http://orcid.org/0000-0002-2656-5291

## REFERENCES

Achenbach, T. (1990). *Infant assessment unit-young adult self report*. Burlington, VT: University of Vermont, Department of Psychiatry.

Achenbach, T. M., & Edelbrock, C. S. (1991). *Youth self-report and profile*. University of Vermont, Department of Psychiatry.

Asperger, H. (1944). Die "Autistischen Psychopathen" im Kindesalter. *Archiv Für Psychiatrie Und Nervenkrankheiten*, 117(1), 76–136.

American Psychiatric Association (2013). *Diagnostic and statistical manual of mental disorders (DSM-5®)*. American Psychiatric Pub.

Bar, M. (2007). The proactive brain: Using analogies and associations to generate predictions. *Trends in Cognitive Sciences*, 11(7), 280–289.

Baron-Cohen, S., Leslie, A. M., & Frith, U. (1985). Does the autistic child have a "theory of mind"? *Cognition*, 21(1), 37–46.

Barrett, L. F. (2017). The theory of constructed emotion: An active inference account of interoception and categorization. *Social Cognitive and Affective Neuroscience*, 12(1), 1–23.

Barrett, L. F., & Satpute, A. B. (2013). Large-scale brain networks in affective and social neuroscience: Towards an integrative functional architecture of the brain. *Current Opinion in Neurobiology*, 23(3), 361–372.

Bastos, A. M., Usrey, W. M., Adams, R. A., Mangun, G. R., Fries, P., & Friston, K. J. (2012). Canonical microcircuits for predictive coding. *Neuron*, 76(4), 695–711.

Bölte, S., Rühl, D., Schmötzer, G., & Poustka, F. (2006). Diagnostisches Interview für Autismus—Revidiert. Deutsche Fassung des Autism Diagnostic Interview—Revised von Michael Rutter, Ann LeCouteur und Catherine Lord, 1. Auflage. Bern: Hans Huber, Hogrefe AG.

Bosl, W., Tierney, A., Tager-Flusberg, H., & Nelson, C. (2011). EEG complexity as a biomarker for autism spectrum disorder risk. *BMC Medicine*, 9, 18.

Brambilla, P., Hardan, A., di Nemi, S. U., Perez, J., Soares, J. C., & Barale, F. (2003). Brain anatomy and development in autism: Review of structural MRI studies. *Brain Research Bulletin*, 61(6), 557–569.

Brock, J. (2012). Alternative Bayesian accounts of autistic perception: Comment on Pellicano and Burr. *Trends in Cognitive Sciences*, 16(12), 573–574.

Brodski-Guerniero, A., Paasch, G.-F., Wollstadt, P., Özdemir, I., Lizier, J. T., & Wibral, M. (2017). Information-theoretic evidence for predictive coding in the face-processing system. *Journal of Neuroscience*, 37(34), 8273–8283.

Buckner, R. L., Andrews-Hanna, J. R., & Schacter, D. L. (2008). The brain's default network. *Annals of the New York Academy of Sciences*, 1124(1), 1–38.

Catarino, A., Churches, O., Baron-Cohen, S., Andrade, A., & Ring, H. (2011). Atypical EEG complexity in autism spectrum conditions: A multiscale entropy analysis. *Clinical Neurophysiology*, 122(12), 2375–2383.

Cherkassky, V. L., Kana, R. K., Keller, T. A., & Just, M. A. (2006). Functional connectivity in a baseline resting-state network in autism. *Neuroreport*, 17(16), 1687–1690.

Christensen, D. L., Baio, J., Van Naarden Braun, K., Bilder, D., Charles, J., Constantino, J. N., ... Yeargin-Allsopp, M. (2016). Prevalence and characteristics of autism spectrum disorder among children aged 8 years — Autism and developmental disabilities monitoring network, 11 sites, United States, 2012. *Morbidity and Mortality Weekly Report. Surveillance Summaries (Washington, D.C. : 2002)*, 65(3), 1.

Clark, A. (2013). Whatever next? Predictive brains, situated agents, and the future of cognitive science. *The Behavioral and Brain Sciences*, 36(3), 181–204.

Cover, T. M., & Thomas, J. A. (2012). *Elements of information theory*. John Wiley & Sons.

Deutsche Child Behavior Checklist (1998a). Fragebogen für Jugendliche; deutsche Bearbeitung der Youth Self-Report Form der Child Behavior Checklist (YSR). Einführung und Anleitung zur Handauswertung mit deutschen Normen, bearbeitet von M. Döpfner, J. Plück, S. Bölte, K. Lenz, P. Melchers & K. Heim (2. Aufl.). Köln: Arbeitsgruppe Kinder-, Jugend- und Familiendiagnostik (KJFD).

Deutsche Child Behavior Checklist (1998b). *Fragebogen für junge Erwachsene (YASR)*. Köln: Arbeitsgruppe Kinder-, Jugend-und Familiendiagnostik (KJFD).

Dienes, Z. (2014). Using Bayes to get the most out of non-significant results. *Frontiers in Psychology*, 5, 781.

Fatemi, S. H., Aldinger, K. A., Ashwood, P., Bauman, M. L., Blaha, C. D., Blatt, G. J., ... Welsh, J. P. (2012). Consensus paper: Pathological role of the cerebellum in autism. *The Cerebellum*, 11(3), 777–807.

Fiser, J., Berkes, P., Orbán, G., & Lengyel, M. (2010). Statistically optimal perception and learning: From behavior to neural representations. *Trends in Cognitive Sciences*, 14(3), 119–130.

Friston, K. (2005). A theory of cortical responses. *Philosophical Transactions of the Royal Society of London. Series B, Biological Sciences*, 360(1456), 815–836.

Friston, K. (2009). The free-energy principle: A rough guide to the brain? *Trends in Cognitive Sciences*, 13(7), 293–301.

Friston, K. (2010). The free-energy principle: A unified brain theory? *Nature Reviews. Neuroscience*, 11(2), 127–138.

Friston, K. J., Lawson, R., & Frith, C. D. (2013). On hyperpriors and hypopriors: Comment on Pellicano and Burr. *Trends in Cognitive Sciences*, 17(1), 1–1016.

Friston, K., & Kiebel, S. (2009). Predictive coding under the free-energy principle. *Philosophical Transactions of the Royal Society of London. Series B, Biological Sciences*, 364(1521), 1211–1221.

Gómez, C., Lizier, J. T., Schaum, M., Wollstadt, P., Grützner, C., Uhlhaas, P., ... Wibral, M. (2014). Reduced predictable information in brain signals in autism spectrum disorder. *Frontiers in Neuroinformatics*, 8, 9.

Grandin, T. (1992). An inside view of autism. *High-Functioning Individuals with Autism*, 105–126.

Gross, J., Baillet, S., Barnes, G. R., Henson, R. N., Hillebrand, A., Jensen, O., ... Oostenveld, R. (2012). Good-practice for conducting and reporting MEG research. *NeuroImage*,

Happé, F., & Frith, U. (2006). The weak coherence account: Detail-focused cognitive style in autism spectrum disorders. *Journal of Autism and Developmental Disorders*, 36(1), 5–25.

Happé, F. G. (1996). Studying weak central coherence at low levels: Children with autism do not succumb to visual illusions. A research note. *Journal of Child Psychology and Psychiatry*, 37(7), 873–877.

Hurlburt, R. T., Happe, F., & Frith, U. (1994). Sampling the form of inner experience in three adults with Asperger syndrome. *Psychological Medicine*, 24(2), 385–395.

Jeffreys, H. (1998). *The theory of probability*. OUP Oxford.

Joseph, R. M., Keehn, B., Connolly, C., Wolfe, J. M., & Horowitz, T. S. (2009). Why is visual search superior in autism spectrum disorder? *Developmental Science*, 12(6), 1083–1096.

Kanner, L. (1943). Autistic disturbances of affective contact. *Nervous Child*, 2, 217–250 [Database].

Kennedy, D. P., Redcay, E., & Courchesne, E. (2006). Failing to deactivate: Resting functional abnormalities in autism. *Proceedings of the National Academy of Sciences of the United States of America*, 103(21), 8275–8280.

Kiebel, S. J., Daunizeau, J., & Friston, K. J. (2008). A hierarchy of time-scales and the brain. *PLoS Computational Biology*, 4(11), e1000209.

Kozachenko, L. F., & Leonenko, N. N. (1987). Sample estimate of the entropy of a random vector. *Problemy Peredachi Informatsii*, 23, 9–16.

Kraskov, A., Stögbauer, H., & Grassberger, P. (2004). Estimating mutual information. *Physical Review E*, 69(6), 066138.

Langton, C. G. (1990). Computation at the edge of chaos: Phase transitions and emergent computation. *Physica D: Nonlinear Phenomena*, 42 (1–3), 12–37.

Lawson, R. P., Rees, G., & Friston, K. J. (2014). An aberrant precision account of autism. *Frontiers in Human Neuroscience*, 8, 302.

Liang, F., Paulo, R., Molina, G., Clyde, M. A., & Berger, J. O. (2008). Mixtures of g priors for Bayesian variable selection. *Journal of the American Statistical Association*, 103(481), 410–423.

Lindner, M., Vicente, R., Priesemann, V., & Wibral, M. (2011). TRENTOOL: A Matlab open source toolbox to analyse information flow in time series data with transfer entropy. *BMC Neuroscience*, 12, 119.

Lizier, J. T. (2014). JIDT: An information-theoretic toolkit for studying the dynamics of complex systems. *Frontiers in Robotics and AI*, 1, 11.

Lizier, J. T., Prokopenko, M., & Zomaya, A. Y. (2012). Local measures of information storage in complex distributed computation. *Information Sciences*, 208, 39–54.

Lord, C., Risi, S., Lambrecht, L., Cook, E. H., Leventhal, B. L., DiLavore, P. C., . . . Rutter, M. (2000). The Autism Diagnostic Observation Schedule—Generic: A standard measure of social and communication deficits associated with the spectrum of autism. *Journal of Autism and Developmental Disorders*, 30(3), 205–223.

Lynch, C. J., Uddin, L. Q., Supekar, K., Khouzam, A., Phillips, J., & Menon, V. (2013). Default mode network in childhood autism: Posteromedial cortex heterogeneity and relationship with social deficits. *Biological Psychiatry*, 74(3), 212–219.

Makeig, S., Bell, A. J., Jung, T.-P., & Sejnowski, T. J. (1996). Independent component analysis of electroencephalographic data. *Advances in Neural Information Processing Systems*, 145–151.

Mason, M. F., Norton, M. I., Van Horn, J. D., Wegner, D. M., Grafton, S. T., Macrae, C. N. (2007). Wandering minds: the default network and stimulus-independent thought. *Science*, 315, 393–395.

Maris, E., & Oostenveld, R. (2007). Nonparametric statistical testing of EEG- and MEG-data. *Journal of Neuroscience Methods*, 164(1), 177–190.

Monk, C. S., Peltier, S. J., Wiggins, J. L., Weng, S.-J., Carrasco, M., Risi, S., & Lord, C. (2009). Abnormalities of intrinsic functional connectivity in autism spectrum disorders. *NeuroImage*, 47(2), 764–772.

Morey, R. D., Rouder, J. N., Jamil, T., & Morey, M. R. D. (2015). Package 'BayesFactor.' ftp://alvarestech.com/pub/plan/R/web/packages/BayesFactor/BayesFactor.pdf

Nolte, G. (2003). The magnetic lead field theorem in the quasi-static approximation and its use for magnetoencephalography forward calculation in realistic volume conductors. *Physics in Medicine and Biology*, 48(22), 3637–3652.

Oldfield, R. C. (1971). The assessment and analysis of handedness: The Edinburgh inventory. *Neuropsychologia*, 9(1), 97–113.

Oostenveld, R., Fries, P., Maris, E., & Schoffelen, J.-M. (2011). FieldTrip: Open source software for advanced analysis of MEG, EEG, and invasive electrophysiological data. *Computational Intelligence and Neuroscience*, 2011, 1.

Pellicano, E., & Burr, D. (2012). When the world becomes "too real": A Bayesian explanation of autistic perception. *Trends in Cognitive Sciences*, 16(10), 504–510.

Percival, D. B., & Walden, A. T. (1993). *Spectral analysis for physical applications*. Cambridge University Press.

Pierce, K., & Courchesne, E. (2001). Evidence for a cerebellar role in reduced exploration and stereotyped behavior in autism. *Biological Psychiatry*, 49(8), 655–664.

Plaisted, K., O'Riordan, M., & Baron-Cohen, S. (1998). Enhanced discrimination of novel, highly similar stimuli by adults with autism during a perceptual learning task. *Journal of Child Psychology and Psychiatry*, 39(5), 765–775.

Ragwitz, M., & Kantz, H. (2002). Markov models from data by simple nonlinear time series predictors in delay embedding spaces. *Physical Review E*, 65(5), 056201.

Raichle, M. E. (2015). The brain's default mode network. *Annual Review of Neuroscience*, 38, 433–447.

Rao, R. P. N., & Ballard, D. H. (1999). Predictive coding in the visual cortex: A functional interpretation of some extra-classical receptive-field effects. *Nature Neuroscience*, 2(1), 79–87.

R Core Team (2016). *A language and environment for statistical computing*. Vienna, Austria: R Foundation for Statistical Computing.

Rouder, J. N., & Morey, R. D. (2012). Default Bayes factors for model selection in regression. *Multivariate Behavioral Research*, 47(6), 877–903.

Rühl, D., Bölte, S., Feineis-Matthews, S., & Poustka, F. (2004). *Diagnostische Beobachtungsskala für Autistische Störungen*. Deutsche Fassung der Autism Diagnostic Observation Schedule. Hans Huber, Hogrefe AG, Bern.

Russell, J. E. (1997). *Autism as an executive disorder*. Oxford University Press.

Rutter, M.,L., Couteur, A., & Lord, C. (2003). Autism diagnostic interview-revised. *Los Angeles CA Western Psychological Services*, 29, 30.

Sadaghiani, S., Hesselmann, G., Friston, K. J., & Kleinschmidt, A. (2010). The relation of ongoing brain activity, evoked neural responses, and cognition. *Frontiers in Systems Neuroscience*, 4, 20.

Shah, A., & Frith, U. (1983). An islet of ability in autistic children: A research note. *Journal of Child Psychology and Psychiatry, and Allied Disciplines*, 24(4), 613–620.

Shannon, C. E. (2001). A mathematical theory of communication. *ACM SIGMOBILE Mobile Computing and Communications Review*, 5(1), 3–55.

Sinha, P. (2002). Qualitative representations for recognition. In: *Biologically motivated computer vision* (pp. 249–262). Springer. http://link.springer.com/chapter/10.1007/3-540-36181-2_25

Slepian, D. (1978). Prolate spheroidal wave functions, Fourier analysis and uncertainty. *Bell System Technical Journal*, 57(5), 1371–1429.

Van de Cruys, S., Evers, K., Van der Hallen, R., Van Eylen, L., Boets, B., de-Wit, L., & Wagemans, J. (2014). Precise minds in uncertain worlds: Predictive coding in autism. *Psychological Review*, 121(4), 649.

Van Veen, B. D., Van Drongelen, W., Yuchtman, M., & Suzuki, A. (1997). Localization of brain electrical activity via linearly constrained minimum variance spatial filtering. *IEEE Transactions on Bio-Medical Engineering*, 44(9), 867–880.

Wagner, A. D., Shannon, B. J., Kahn, I., & Buckner, R. L. (2005). Parietal lobe contributions to episodic memory retrieval. *Trends in Cognitive Sciences*, 9(9), 445–453.

Waiter, G. D., Williams, J. H. G., Murray, A. D., Gilchrist, A., Perrett, D. I., & Whiten, A. (2004). A voxel-based investigation of brain structure in male adolescents with autistic spectrum disorder. *NeuroImage*, 22(2), 619–625.

Washington, S. D., Gordon, E. M., Brar, J., Warburton, S., Sawyer, A. T., Wolfe, A., . . . Van Meter, J. W. (2014). Dysmaturation of the default mode network in autism. *Human Brain Mapping*, 35(4), 1284–1296.

Weiß, R. H. (2006). Grundintelligenztest skala 2—revision CFT 20-R [culture fair intelligence test scale 2—revision]. Hogrefe Gött.

Weng, S.-J., Wiggins, J. L., Peltier, S. J., Carrasco, M., Risi, S., Lord, C., & Monk, C. S. (2010). Alterations of resting state functional connectivity in the default network in adolescents with autism spectrum disorders. *Brain Research*, 1313, 202–214.

Whitfield-Gabrieli, S., & Ford, J. M. (2012). Default mode network activity and connectivity in psychopathology. *Annual Review of Clinical Psychology*, 8, 49–76.

Wibral, M., Lizier, J. T., & Priesemann, V. (2015). Bits from brains for biologically-inspired computing. *Frontiers in Robotics and AI*, 2, http://journal.frontiersin.org/article/10.3389/frobt.2015.00005/pdf.

Wibral, M., Lizier, J. T., Vögler, S., Priesemann, V., & Galuske, R. (2014). Local active information storage as a tool to understand distributed neural information processing. *Frontiers in Neuroinformatics*, 8, 1.

Wollstadt, P., Sellers, K. K., Rudelt, L., Priesemann, V., Hutt, A., Fröhlich, F., & Wibral, M. (2017). Breakdown of local information processing may underlie isoflurane anesthesia effects. *PLoS Computational Biology*, 13(6), e1005511.

World Health Organization (1992). The ICD-10 classification of mental and behavioural disorders: Clinical descriptions and diagnostic guidelines. Geneva: World Health Organization.

Zipser, D., Kehoe, B., Littlewort, G., & Fuster, J. (1993). A spiking network model of short-term active memory. *Journal of Neuroscience*, 13(8), 3406–3420.

## SUPPORTING INFORMATION

Additional Supporting Information may be found online in the supporting information tab for this article.